# Optimum filter-based discrimination of neutrons and gamma rays

**Amiri, M., Prenosil, V. & Cvachovec, F.**



**Original citation & hyperlink:**
[Amiri, M, Prenosil, V & Cvachovec, F 2015, Optimum filter-based discrimination of neutrons and gamma rays. in 4th International Conference on Advancements in Nuclear Instrumentation Measurement Methods and their Applications (ANIMMA). IEEE, Advancements in Nuclear Instrumentation Measurement Methods and their Applications, Lisbon, Portugal, 20/04/15.
https://dx.doi.org/10.1109/ANIMMA.2015.7465552

DOI 10.1109/ANIMMA.2015.7465552
ISBN 978-1-4799-9918-7

Publisher: IEEE

# Optimum Filter-Based Discrimination of Neutrons and Gamma Rays

Moslem Amiri, Václav Přenosil, and František Cvachovec

***Abstract*—An optimum filter-based method for discrimination of neutrons and gamma-rays in a mixed radiation field is presented. The existing filter-based implementations of discriminators require sample pulse responses in advance of the experiment run to build the filter coefficients, which makes them less practical. Our novel technique creates the coefficients during the experiment and improves their quality gradually. Applied to several sets of mixed neutron and photon signals obtained through different digitizers using stilbene scintillator, this approach is analyzed and its discrimination quality is measured.**

***Index Terms*—Counter/discriminator, optimum filter, neutron spectroscopy, organic scintillator.**

## I. Introduction

THIS article deals with the measurement and discrimination of neutron and $\gamma$-ray radiations. The primary reaction producing neutron field and scattering reactions of neutrons with materials in the environment lead to the production of $\gamma$-ray as a background radiation. It is often necessary to measure neutron radiation in mixed fields of high $\gamma$-ray intensity. Certain scintillators could effectively discriminate between neutron and $\gamma$ radiation; their scintillation pulse shapes for these two radiations are different from each other. The differing pulse shapes of neutrons and $\gamma$-rays is the result of different de-excitation delays in the scintillator when these particles strike it. A composite pulse curve often comprises a fast and a slow component of scintillation. The long-lived slow component often reveals the nature of the particle striking the detector. This fact is usually used to separate different kinds of particles; this process is called pulse shape discrimination (PSD) [1]. PSD techniques are mainly used to discriminate neutrons from the $\gamma$-rays.

Organic scintillation detectors are widely used for neutron detection and spectroscopy. Among organic scintillators, stilbene and NE-213 are favored; they have rather low light output per unit energy, but this light output induced by charged protons can be easily distinguished from electrons/photons. Hence, stilbene and NE-213 scintillators produce very good results using PSD methods.

Although analog PSD techniques (e.g. rise-time inspection, zero-crossing method, and charge comparison [2]) make acceptable n/$\gamma$-ray discrimination, availability of precise and fast digitizers and various PSD algorithms have made it possible to do a better discrimination of these radiations digitally. Among digital PSD methods, pulse rise-time algorithm and charge comparison are probably the most favorable ones.

In this paper, the original optimum filter-based n/$\gamma$-ray discrimination method is introduced first and its separation quality is calculated. Since the original implementation is far from practical, an update to this filter-based method is introduced later in this article and compared to the original implementation. To obtain the sampled data of mixed neutron and $\gamma$-ray pulses, two differently-featured digitizers (explained in Section II) are used which differ mainly in their sampling rate and output quantization level resolution. Doing so, the effect of resolution and sampling frequency of the digitizers on the quality of the discrimination result for the methods discussed in this article could be found. Every experiment is carried out under the same experimental conditions, using 100,000 pulses of mixed neutron and photon signals. For this work, the field consists of mostly $\gamma$-rays and some neutrons.

A comparison among various techniques, applied to data obtained from the different digitizer types and settings, is done by using the Figure of Merit (FoM) for the n/$\gamma$-ray discrimination, defined as:

$$FoM = \frac{S}{FWHM_n + FWHM_\gamma} \tag{1}$$

where $S$ is the separation between the peaks of the two events, $FWHM_\gamma$ is the full-width half-maximum (FWHM) of the spread of events classified as $\gamma$-rays and $FWHM_n$ is the FWHM of the spread in the neutron peak [3]. FWHMs are calculated using the Gaussian fits to the neutron and $\gamma$-ray events on experimental distribution plot.

## II. Experimental Setup

For this work, stilbene scintillation detector was used with 45x45 crystal, and the neutron-gamma radiation source used was 252Cf(sf). A typical scintillation detector consists of a scintillator and a photomultiplier. The latter is employed to change weak light signals impinging to photocathode (generated by the scintillator) into electric impulses. We used the photomultiplier RCA7265 [4] throughout these experiments. The block diagram of our digital apparatus is shown in Fig. 1.

A preamplifier is selected so as to match the detector output impedance. Two variants of the anode load resistance were tested in conjunction with the organic scintillation detectors. In the first variant, a load resistance of 40 $k\Omega$ was used. A preamplifier matched it to the coaxial cable whose characteristic impedance was 50 $\Omega$. In this case, the different waveforms

Manuscript received May 31, 2015. This work was supported by Technology Agency of the Czech Republic under contract No. TA01011383/2011.

M. Amiri is with the Faculty of Informatics, Masaryk University, Botanicka 68a, 602 00 Brno, Czech Republic (e-mail: amiri@mail.muni.cz).

V. Prenosil is with the Faculty of Informatics, Masaryk University, Botanicka 68a, 602 00 Brno, Czech Republic (e-mail: prenosil@fi.muni.cz).

F. Cvachovec is with the Faculty of Military Technology, University of Defence, Kounicova 156/65, 662 10 Brno, Czech Republic (e-mail: frantisek.cvachovec@unob.cz).

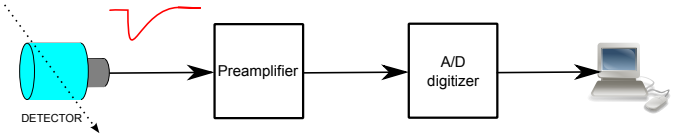


Fig. 1. Block diagram of a digital two-parameter analyzer.

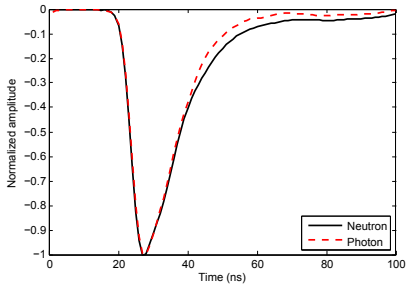


Fig. 2. Comparison of a sample smoothed neutron with a sample smoothed photon. These signals are obtained from the stilbene scintillator.

of the neutron and photon pulses can be detected in the voltage pulse leading edge. If the magnitude of the load resistance is selected to be close to the characteristic impedance of the coaxial cable, which is 50 Ω, the different shapes of the neutron/photon pulses will appear to take effect during the decay time. In this case, no preamplifier is necessary. The latter option was employed here.

Two commercially available Agilent digitizers were used to digitize the output pulses: Acqiris DP210 with 8-bit resolution and set at 1 and 2 GS/s, and Acqiris DC440 with 12-bit resolution and set at 250 and 420 MS/s. While real-time digitizers are also employed in industry today, we used these specific commercial digitizers to study the effects of their various data resolution and sampling frequency features on digital processing.

## III. Neutron and Photon Signals

A sample smoothed neutron is compared with a sample smoothed photon pulse in Fig. 2. These signals are obtained from the stilbene scintillator. As seen in this Figure, these signals are composed of a leading and a trailing edge. The leading edges could not be exploited for discrimination purposes. On the other hand, the trailing edge of the neutron signal takes longer to decay than that of the photon signal. This property could be used to separate these two radiations. However, this difference is not large enough to be easily exploited by directly applying signal processing techniques.

An innovative discrimination approach is to remove the similar segments of the two signal types and apply the technique only to the differing segments.

## IV. Optimum Filter Implementation

In this section, we will use a known principle to implement an optimum filter for discrimination purposes. The principle used here is introduced in [5]. Let $n(i)$ and $g(i)$ be two discrete-time functions, both normalized to unity, i.e.

$$\sum_i n(i) = \sum_i g(i) = 1 \tag{2}$$

If we compute the time function of the relative difference between $n(i)$ and $g(i)$ (weights) as follows:

$$p(i) = \frac{g(i) - n(i)}{g(i) + n(i)} \tag{3}$$

then an unknown function $u(i)$, close to either $n(i)$ or $g(i)$, can be identified as one of them by the sign of $S$ defined as:

$$S = \sum_i p(i)u(i) \tag{4}$$

We use this principle to design a filter for discrimination of neutrons and $\gamma$-rays. In (2), (3), and (4), if we replace $n(i)$ and $g(i)$ with neutron and $\gamma$-ray pulses, respectively, then if $S < 0$, the particle is identified as $\gamma$-ray, and if $S > 0$, as neutron.

According to (3), those parts of the neutron and photon signals that differ most will have greater weights and the similar parts will have negligible weights. The similar segments could have weights with large absolute values when they are very close to zero; but according to (4), the final effect is minimal. Since the leading edges and the end-tail segments of neutrons and $\gamma$-rays have almost the same shape, there will be insignificant weights or effects for corresponding points when these segments are included. However this minimal improvement of the discrimination caused by these segments will help us better identify the particles in low energy region. Inclusion of these parts is directly related to the capabilities of the hardware at hand. Omitting these segments will have the benefit of fewer number of multiplications (based on (4)), but a slight decrease in the quality of the results. For this work, the area of interest starts from the point where the leading edge hits the 1% threshold level and the end point is a constant number of samples after this starting point for all signals, such that this interval covers a signal as much as possible.

In (3), a sample $\gamma$-ray $g(i)$ and a sample neutron $n(i)$ are picked and used to build the weights. These samples need to be patterns representing the types of pulses contained in the whole data set. Therefore, more than one sample should be used for each pulse type to obtain better results. If we use $k$ number of pulses ($k > 1$) from each radiation type to build the sample pulses required, then

$$\begin{aligned} g(i) &= \frac{\sum_{j=1}^{k} g_j(i)}{k} \\ n(i) &= \frac{\sum_{j=1}^{k} n_j(i)}{k} \end{aligned} \tag{5}$$

Once every point of the two sample pulses are built using (5), they are normalized to unity using (2) (as Fig. 3 illustrates), and then applied to (3) to build the weight sequence (as shown in Fig. 4).

We use the constant weight sequence $p(i)$, in conjunction with every arriving pulse, to detect that specific pulse. If $u(i)$ is the unknown pulse to be processed, it is passed along with $p(i)$ to (4) to compute $S$. As mentioned before, $S$ serves as the identifier for the pulse and hence can be used as counting/discriminating factor. The sign of $S$ for a pulse reveals its identity; using (3), neutrons will have positive signs for $S$ while photons will have negative ones. This can be used

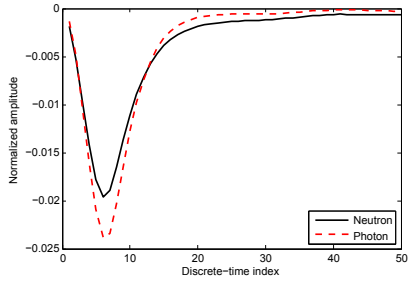


Fig. 3. Segments of neutron and $\gamma$-ray pulses, obtained from DC440 digitizer (12-bit resolution, 420 MS/s), when normalized to unity (using (2)).

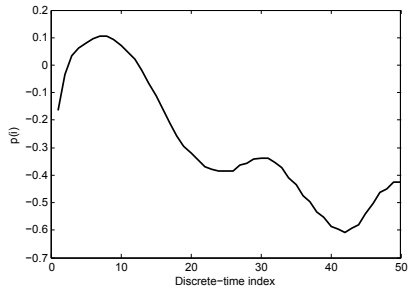


Fig. 4. Weight function $p(i)$, obtained from (3), using the two signal segments shown in Fig. 3.

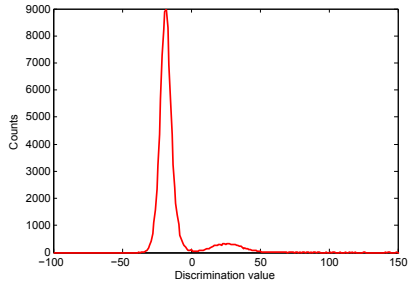


Fig. 5. Discrimination of photon and neutron signals, applying the original optimum filter-based method. The pulses are obtained using DC440 digitizer (12-bit resolution, 420 MS/s).

to count the number of neutrons and photons in an experiment. Since the zero base-line is the separator between these signals, to find the efficiency of discrimination, an ideal factor to use would be the amplitude of $S$ for a pulse.

Fig. 5 illustrates the experimental distribution plot of neutrons and photons for the data obtained from DC440 digitizer with 12-bit resolution and set at 420 MS/s frequency rate. As seen, the zero discrimination value is the separator here; neutrons have positive and $\gamma$-rays have negative discrimination values. FoMs and neutron/photon counts for various data sets with different resolutions and frequency rates are shown in Table I. This method discriminates both low- and high-resolution pulses very efficiently.

## V. Optimum Filter Design with Run-Time Template Buildup

The approach introduced in Section IV discriminates neutrons and $\gamma$-rays very efficiently. However, it requires sample pulse responses in advance of the experiment run to build the filter coefficients. This requirement makes practical implementation of this method difficult; typically another discrimination approach should be employed to capture samples of neutrons and $\gamma$-rays before running the filter-based method. An update to the original filter-based discrimination is introduced in [6] which still requires the templates to be available before the discrimination process. In this section, we introduce a novel approach which creates the coefficients during the experiment and improves their quality gradually.

TABLE I
FoMs and counts of the pulses obtained from DC440 and DP210 digitizers under different sampling rates, when the original optimum filter-based discrimination method is used.

| Data format | FoM | Neutron counts | Photon counts |
|---|---|---|---|
| **12-bit, 250 MS/s** | 1.25 | 9032 | 90968 |
| **12-bit, 420 MS/s** | 1.21 | 9293 | 90707 |
| **8-bit, 1 GS/s** | 1.06 | 9558 | 90442 |
| **8-bit, 2 GS/s** | 1.05 | 9462 | 90538 |

For every pulse captured in this experiment, only the trailing edge (starting from the peak) of the pulse is processed or recorded. For the experimental setup explained in Section II, this segment could cover the interval of 37 $ns$ after the peak minimum, or the interval of 110 $ns$ after the peak maximum, or even beyond. However, if the resolution is low, or the noise level is high, this segment should be short, especially when the sampling rate is high. Cutting short the end-tail segment will eliminate the negative effect of anomalies in the long tail on the count/discrimination process.

Fig. 6 illustrates the steps needed to implement our method to discriminate and count the pulse types. These steps are explained in the following:

1) The first captured pulse is considered template 1 ($T_1(i)$) and stored. $T_1(i)$ is normalized to unity and recorded ($t_1(i)$);
2) The second pulse is considered template 2 ($T_2(i)$), stored, and then normalized to unity ($t_2(i)$) and recorded for future use;
3) The next arriving pulse ($X(i)$) is treated as a template; it is stored and then normalized to unity ($x(i)$). Having three templates now, the following weight functions are calculated:

$$pt_1(i) = \frac{x(i) - t_1(i)}{x(i) + t_1(i)} \qquad pt_2(i) = \frac{t_2(i) - x(i)}{t_2(i) + x(i)} \tag{6}$$

4) The weight functions built in step 3 are used to identify $X(i)$ through the following equations:

$$St_1 = C_1 \cdot \sum_i pt_1(i) \cdot X(i) \qquad St_2 = C_2 \cdot \sum_i pt_2(i) \cdot X(i) \tag{7}$$

$C_1$ and $C_2$ coefficients could be either $+1$ or $-1$. This setting is dependent on weight functions (6): if the numerator is the subtraction of neutron sequence from photon sequence (photon sequence from neutron

sequence), the corresponding coefficient must be $+1$ ($-1$). A normalized photon signal has larger magnitude at the peak point than a normalized neutron (this is evident in Fig. 3). This feature makes a weight function, (6), positive at the peak point when the numerator is the subtraction of neutron sequence from photon sequence, and negative when the opposite order is on the numerator. As mentioned before, to simplify this technique, we start capturing signals from the peak of the pulses. Therefore, in order to find the value of a coefficient, only the first sample of the corresponding weight function sequence needs to be checked; if $pt_1(1) < 0$ then $C_1 = -1$, otherwise $C_1 = +1$. The same rule applies to $pt_2$ and $C_2$.

5) If absolute value of $St_1$ is greater than that of $St_2$, template 2 ($T_2(i)$) needs to be updated; in our implementation, every sample in $T_2(i)$ retains $9/10$th of its old value while receiving $1/10$th from $X(i)$. If $St_1$ is positive, it is counted as neutron, otherwise photon. Moreover, $St_1$ itself is treated as a discrimination factor. $T_2(i)$ is then normalized to unity and stored in $t_2(i)$. On the other hand, if absolute value of $St_2$ is greater, template 1 ($T_1(i)$) needs to be updated; every sample in $T_1(i)$ retains $9/10$th of its old value while receiving $1/10$th from $X(i)$. If $St_2$ is positive, it is counted as neutron, otherwise photon. $St_2$ is also used as a good discrimination factor. $T_1(i)$ is then normalized to unity and stored in $t_1(i)$.
6) For every arriving pulse $X(i)$, the steps 3 to 5 are repeated.

There are eight possible conditions which could occur in this introduced algorithm; any of $T_1(i)$, $T_2(i)$, or $X(i)$ could be either neutron ($n$) or gamma-ray ($\gamma$). In order to elaborate on this method, all these cases are reviewed here:

1) $T_1(i) = n$, $X(i) = n$, $T_2(i) = \gamma$
$\rightarrow St_1 \approx 0$, $C_2 = +1$, $St_2 > 0$
Therefore, $T_1(i)$ ($= n$) is updated with $X(i)$ ($= n$), and a neutron is counted.
2) $T_1(i) = n$, $X(i) = \gamma$, $T_2(i) = \gamma$
$\rightarrow C_1 = +1$, $St_1 < 0$, $St_2 \approx 0$
Therefore, $T_2(i)$ ($= \gamma$) is updated with $X(i)$ ($= \gamma$), and a photon is counted.
3) $T_1(i) = \gamma$, $X(i) = n$, $T_2(i) = n$
$\rightarrow C_1 = -1$, $St_1 > 0$, $St_2 \approx 0$
Therefore, $T_2(i)$ ($= n$) is updated with $X(i)$ ($= n$), and a neutron is counted.
4) $T_1(i) = \gamma$, $X(i) = \gamma$, $T_2(i) = n$
$\rightarrow St_1 \approx 0$, $C_2 = -1$, $St_2 < 0$
Therefore, $T_1(i)$ ($= \gamma$) is updated with $X(i)$ ($= \gamma$), and a photon is counted.
5) $T_1(i) = \gamma$, $X(i) = n$, $T_2(i) = \gamma$
$\rightarrow C_1 = -1$, $St_1 > 0$, $C_2 = +1$, $St_2 > 0$
This condition, where both $T_1(i)$ and $T_2(i)$ are of the same signal type but $X(i)$ is different, could occur only at the beginning of the experiment and this method resolves it immediately. Here, $St_1$ and $St_2$ have almost the same value, but when compared, one is larger than the other. If $St_1$ is larger, $T_2(i)$ ($= \gamma$) will be updated with $X(i)$ ($= n$), and a neutron will be counted. However, if $St_2$ is larger, $T_1(i)$ ($= \gamma$) will be updated with $X(i)$ ($= n$), and a neutron will be counted. Therefore, since both templates $T_1(i)$ and $T_2(i)$ are $\gamma$ (which is basically incorrect and should be fixed), one of these templates will be randomly forced to be updated with $n$ and hence the two templates will be gradually made different. This is exactly what we expect to happen in order for the algorithm to work correctly.
6) $T_1(i) = \gamma$, $X(i) = \gamma$, $T_2(i) = \gamma$
$\rightarrow St_1 \approx 0$, $St_2 \approx 0$
This condition, where $T_1(i)$ and $T_2(i)$ and $X(i)$ are all the same signal type, could occur only at the very beginning of the experiment. Here, $St_1$ and $St_2$ are almost zero both, but when compared, one is larger than the other. As a result, one of the templates $T_1(i)$ ($= \gamma$) or $T_2(i)$ ($= \gamma$) will randomly be updated with $X(i)$ ($= \gamma$). This update has no negative effect. However, $X(i)$ will be randomly counted as either neutron or photon. This is a rare erroneous condition (along with 7th case below) of this method which could happen as long as the same pulse type is received at the start of the experiment. As soon as a different type of radiation $X(i)$ is received, 5th case above is fulfilled and the algorithm gradually fixes the templates' sequences, pulse counts, and discrimination process.
7) $T_1(i) = n$, $X(i) = n$, $T_2(i) = n$
$\rightarrow St_1 \approx 0$, $St_2 \approx 0$
This is similar to the 6th condition above where $T_1(i)$ and $T_2(i)$ and $X(i)$ are all of the same radiation type. As mentioned, this could occur only at the very beginning of the experiment. One template, $T_1(i)$ ($= n$) or $T_2(i)$ ($= n$) will randomly be updated with $X(i)$ ($= n$), with no special effect. However, $X(i)$ will be randomly counted as either neutron or photon. When a different type of radiation $X(i)$ is captured, the algorithm will enter its self-correcting phase.
8) $T_1(i) = n$, $X(i) = \gamma$, $T_2(i) = n$
$\rightarrow C_1 = +1$, $St_1 < 0$, $C_2 = -1$, $St_2 < 0$
This is a condition similar to 5th case above where both $T_1(i)$ and $T_2(i)$ are the same signal type but $X(i)$ is different. As mentioned, this could occur only at the beginning of the experiment and this method resolves this condition. If $St_1$ is larger, $T_2(i)$ ($= n$) will be updated with $X(i)$ ($= \gamma$), and if $St_2$ is larger, $T_1(i)$ ($= n$) will be updated with $X(i)$ ($= \gamma$). Hence the two templates, $T_1(i)$ and $T_2(i)$, will be gradually made different. In either situation, a photon will correctly be counted.

Fig. 7 illustrates the experimental distribution plot of neutrons and photons for the data obtained from DC440 digitizer with 12-bit resolution and set at 420 MS/s frequency rate. Similar to the plot shown in Fig. 5, the zero discrimination value is the separator; neutrons have positive and $\gamma$-rays have negative discrimination values. FoMs and neutron/photon counts for various data sets with different resolutions and

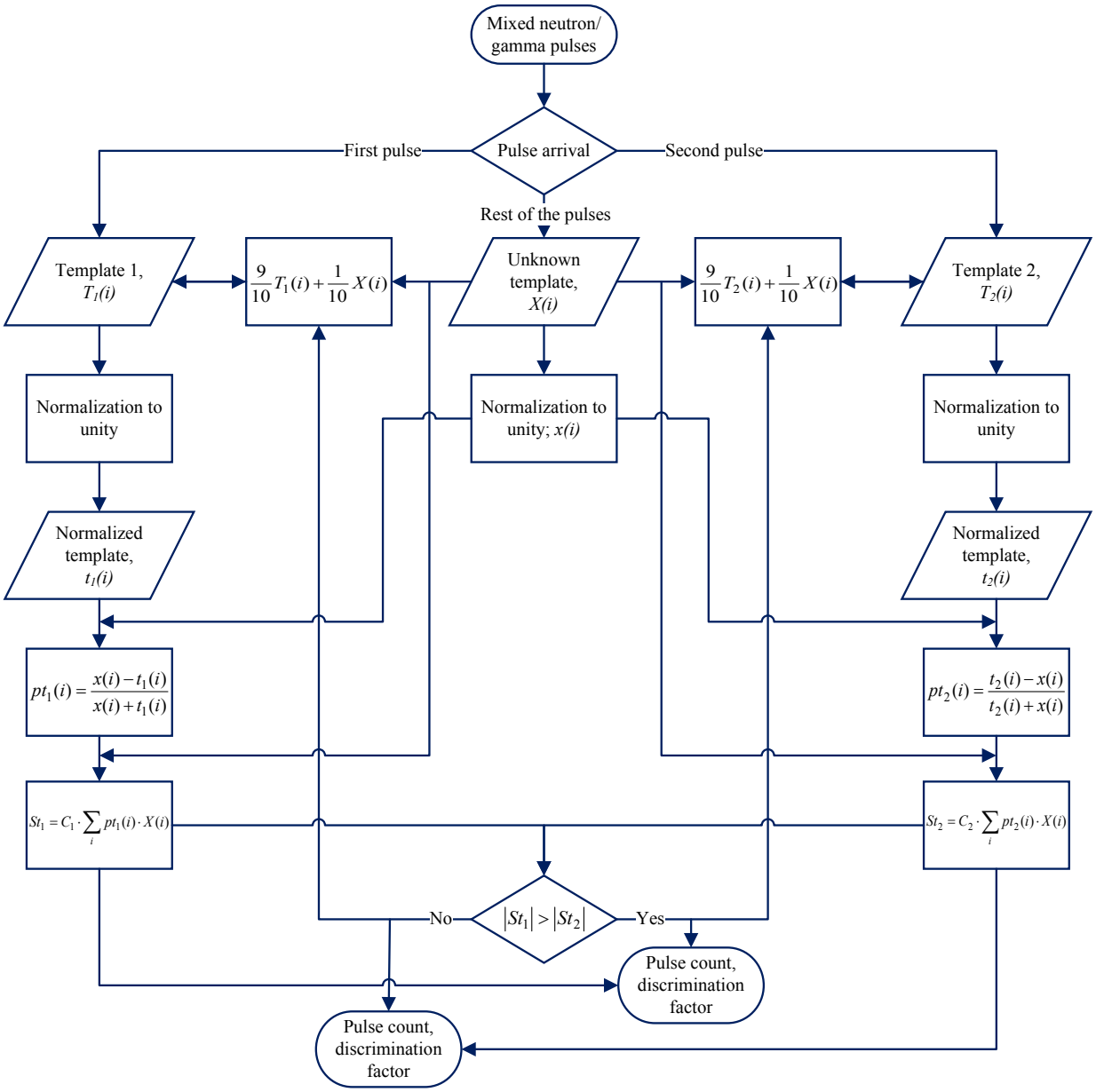


Fig. 6. The proposed algorithm for optimum filter design with run-time template buildup. The details of steps taken in this algorithm are given in Section V.

TABLE II
FOMS AND COUNTS OF THE PULSES OBTAINED FROM DC440 AND DP210 DIGITIZERS UNDER DIFFERENT SAMPLING RATES. OPTIMUM FILTER-BASED METHOD WITH RUN-TIME TEMPLATE BUILDUP IS APPLIED TO THE DATA.

| Data format | FoM | Neutron counts | Photon counts |
|---|---|---|---|
| **12-bit, 250 MS/s** | 1.24 | 9494 | 90506 |
| **12-bit, 420 MS/s** | 1.28 | 9286 | 90714 |
| **8-bit, 1 GS/s** | 1.08 | 9533 | 90467 |
| **8-bit, 2 GS/s** | 0.99 | 9617 | 90383 |

frequency rates are shown in Table II. The same data sets used for the experiments of Section IV are used here for comparison purposes. This method discriminates pulses very well, with DC440 digitizer (12-bit resolution, and set at 420 MS/s) showing the highest efficiency.

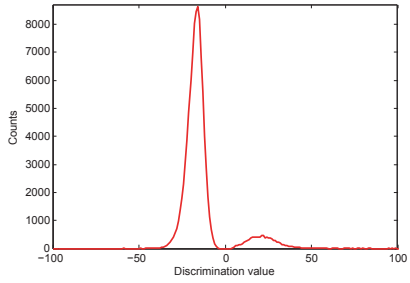


Fig. 7. Discrimination of photon and neutron signals, applying optimum filter-based method with run-time template buildup. The pulses are obtained using DC440 digitizer (12-bit resolution, 420 MS/s).

## VI. DISCUSSION

To update template 1 ($T_1(i)$) or template 2 ($T_2(i)$) in our implementation, every sample in the template retains $9/10$th

TABLE III
COUNT ERROR RATES OF THE PULSES OBTAINED FROM DC440 AND DP210 DIGITIZERS UNDER DIFFERENT SAMPLING RATES.

| Data format | Pulse count error rate |
|---|---|
| **12-bit, 250 MS/s** | 0.462 % |
| **12-bit, 420 MS/s** | 0.007 % |
| **8-bit, 1 GS/s** | 0.025 % |
| **8-bit, 2 GS/s** | 0.155 % |

of its old value while receiving $1/10$th from the arriving pulse $X(i)$. This approach keeps a history of the templates and assures that irregular and out-of-shape pulses will not have their ill-effects on the templates; the templates will recover quickly from the small effects in such cases. If it is expected that the experimental condition will possibly create an abundance of irregular pulses in a row, the ratio of 0.9:0.1 can be made even higher; the side effect of this setting will be a slower template buildup at the beginning of the experiment.

If the approach of Section IV is assumed to count pulse types correctly due to the availability of accurate templates and hence weight sequence in this method, the results obtained through this method could be used as a base to measure the efficiency of the other updating methods. Since the same data sets were used to obtain the results shown in both Tables I and II, the neutron and photon counts in these Tables could be compared; the error rates are listed in Table III. As seen in this Table, a higher resolution with adequate frequency rate (12-bit resolution and 420 MS/s sampling rate in this Table) provides the most accurate pulse count result. The following reasons in the method of Section V could lead to the pulse count differences:

- Capture of the same pulse type at the beginning of experiment, therefore delaying proper template buildup;
- Irregular or noisy pulses which set $C_1$ and $C_2$ coefficients in (7) incorrectly;
- Gradual adaptation of templates; in fact the gradual modification in templates could better the templates throughout the experimental run (especially when the acquisition of pulses occurs within a long time interval) when the environment or the physical apparatus are affected. One could argue that in such a case, the method of Section V should be used as the base and the approach of Section IV as the one deviating from the norm.

It is worth noting that a higher FoM cannot always be associated with a more accurate pulse count, nor a lower FoM with an inaccurate pulse count.

Sampling rate of the digitizer can affect discrimination quality of a method. The FFT of neutron and photon signals indicates frequency components up to 100 MHz [7]. Hence, according to Nyquist criterion, the minimum sampling frequency for neutron and photon signals is about 200 MS/s. Estimating the exact impact of the sampling rate on the separation quality of a method can be involved. For the approaches introduced in this article, as Tables I and II show, increasing from the low sampling rate of 250 MHz to 420 MHz or increasing from the high sampling rate of 1 GHz to 2 GHz does not necessarily improve the FoM.

The factor with a greater impact on discrimination quality

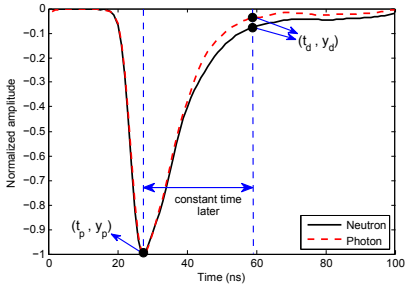


Fig. 8. The points on smoothed neutron and photon signals used in PGA discrimination method.

TABLE IV
FOMS OF PGA METHOD FOR THE PULSES OBTAINED FROM VARIOUS DIGITIZERS.

| Digitizer | 8-bit, 1 GS | 8-bit, 2 GS | 12-bit, 250 MS | 12-bit, 420 MS |
|---|---|---|---|---|
| **FoM** | 0.88 | 0.91 | 0.94 | 1.00 |

is digitizer resolution. The quality of the digitizer output could be measured by signal-to-quantization noise ratio (SQNR). Since quantization errors of neutron and photon signals are almost uniformly distributed over the quantization interval, the following well-known equation [8] reliably estimates the quality of a $b$-bit digitizer output:

$$SQNR(dB) = 1.76 + 6.02b \tag{8}$$

Equation (8) implies that SQNR increases approximately 6 dB for every bit added to the digitizer word length. This relationship gives the number of bits required by an application to assure a given signal-to-noise ratio.

In order to verify the performance of the methods introduced in this article, we apply PGA method to the same pulse data sets as used for the methods in this paper. PGA method, introduced in [3], is recognized as an efficient n/γ-ray discrimination method; the gradient between the peak amplitude and the amplitude a specified time after the peak amplitude (called the discrimination amplitude) on the trailing edge of the pulses are compared and used as the discrimination factor. Fig. 8 illustrates the peak and discrimination amplitudes on neutron and photon signals. The gradient is calculated using

$$m = \frac{\Delta y}{\Delta t} = \frac{(y_p - y_d)}{(t_p - t_d)} \tag{9}$$

where $m$, $y_p$, $y_d$, $t_p$, and $t_d$ are the gradient, the peak amplitude (which is a constant for normalized pulses), the discrimination amplitude, the time of peak amplitude occurrence, and the time of discrimination amplitude occurrence, respectively. For this work, we used some training pulses to locate the best discrimination amplitude, which occurred about 36 $ns$ after the peak of the pulse. The FoMs obtained are listed in Table IV. A comparison shows that the novel methods introduced here have better discrimination qualities than the PGA method does. Fig. 9 shows the best discrimination plot obtained by PGA method.

## VII. CONCLUSION

In this article, an optimum filter-based n/γ-ray discrimination approach was first introduced. This algorithm counts

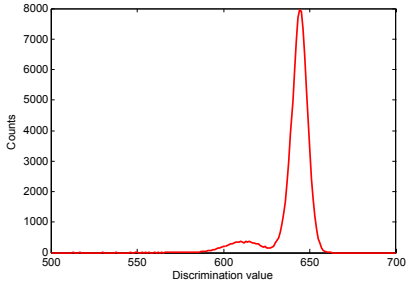


Fig. 9. Discrimination of photon and neutron signals, applying PGA method. The pulses are obtained using DC440 digitizer (12-bit resolution, 420 MS/s).

and discriminates the pulses in a mixed environment very efficiently, however, it requires sample neutron and $\gamma$-ray pulses in advance of the experiment run to build the filter weight sequence. This requirement leads to the employment of another technique prior to the filter-based method to provide proper templates. Since this is not practically acceptable, an improvement to the original optimum filter-based method is made in this article to build the templates during run time. As more pulses are captured, the templates and hence the weight sequences are made finer. This new approach has also the capability to adapt itself to any physical or environmental changes.

Two digitizers, each featuring a different resolution and each set at two different sampling rates, were used to observe the reaction of the methods to the data sampling conditions. The introduced methods are robust, i.e. they provide promising results when applied to the data recorded at either low or high resolutions, or sampled at low or high rates.

## REFERENCES

[1] G. F. Knoll, *Radiation Detection and Measurement*, 3rd ed. New York: Wiley, 2000, ch. 8, p. 230.

[2] G. Ranucci, "An analytical approach to the evaluation of the pulse shape discrimination properties of scintillators," *Nuclear Instruments and Methods in Physics Research Section A: Accelerators, Spectrometers, Detectors and Associated Equipment*, vol. 354, no. 2-3, pp. 389 – 399, 1995. [Online]. Available: http://www.sciencedirect.com/science/article/pii/0168900294008868

[3] B. Mellow, M. Aspinall, R. Mackin, M. Joyce, and A. Peyton, "Digital discrimination of neutrons and g-rays in liquid scintillators using pulse gradient analysis," *Nuclear Instruments and Methods in Physics Research Section A*, vol. 578, no. 1, pp. 191–197, 2007.

[4] "Rca 7265 photomultiplier tube 2" 14-stage s-20," http://www.hofstragroup.com/product/rca-7265-photomultiplier-tube-2-14-stage-s-20/, accessed: 2014-07-15.

[5] E. Gatti and F. de Martini, "A new linear method of discriminating between elementary particles in scintillation counters," in *Int. Symp. Nuclear Electronics*, vol. 2, Belgrade, 1961, pp. 265 – 276.

[6] M. Amiri, V. Přenosil, F. Cvachovec, Z. Matěj, and F. Mravec, "Quick algorithms for real-time discrimination of neutrons and gamma rays," *Journal of Radioanalytical and Nuclear Chemistry*, pp. 1–17, 2014. [Online]. Available: http://dx.doi.org/10.1007/s10967-014-3406-5

[7] F. Belli, B. Esposito, D. Marocco, and M. Riva, "A study on the pulse height resolution of organic scintillator digitized pulses," *Fusion Engineering and Design*, vol. 88, no. 68, pp. 1271 – 1275, 2013, proceedings of the 27th Symposium On Fusion Technology (SOFT-27); Liége, Belgium, September 24-28, 2012. [Online]. Available: http://www.sciencedirect.com/science/article/pii/S092037961200587X

[8] J. G. Proakis and D. G. Manolakis, *Digital Signal Processing, Fourth Edition*. Upper Saddle River, New Jersey 07458: Prentice Hall, 2006.